

Can a Convective Cloud Feedback Help to Eliminate Winter Sea Ice at High CO₂ Concentrations?

DORIAN S. ABBOT

Department of Earth and Planetary Sciences, Harvard University, Cambridge, Massachusetts

CHRIS C. WALKER

FAS-IT Research Computing, Harvard University, Cambridge, Massachusetts

ELI TZIPERMAN

Department of Earth and Planetary Sciences, and School of Engineering and Applied Sciences, Harvard University, Cambridge, Massachusetts

(Manuscript received 24 September 2008, in final form 13 May 2009)

ABSTRACT

Winter sea ice dramatically cools the Arctic climate during the coldest months of the year and may have remote effects on global climate as well. Accurate forecasting of winter sea ice has significant social and economic benefits. Such forecasting requires the identification and understanding of all of the feedbacks that can affect sea ice.

A convective cloud feedback has recently been proposed in the context of explaining equable climates, for example, the climate of the Eocene, which might be important for determining future winter sea ice. In this feedback, CO₂-initiated warming leads to sea ice reduction, which allows increased heat and moisture fluxes from the ocean surface, which in turn destabilizes the atmosphere and leads to atmospheric convection. This atmospheric convection produces optically thick convective clouds and increases high-altitude moisture levels, both of which trap outgoing longwave radiation and therefore result in further warming and sea ice loss.

Here it is shown that this convective cloud feedback is active at high CO₂ during polar night in the coupled ocean–sea ice–land–atmosphere global climate models used for the 1% yr⁻¹ CO₂ increase to the quadrupling (1120 ppm) scenario of the Intergovernmental Panel on Climate Change (IPCC) Fourth Assessment Report. At quadrupled CO₂, model forecasts of maximum seasonal (March) sea ice volume are found to be correlated with polar winter cloud radiative forcing, which the convective cloud feedback increases. In contrast, sea ice volume is entirely uncorrelated with model global climate sensitivity. It is then shown that the convective cloud feedback plays an essential role in the elimination of March sea ice at quadrupled CO₂ in NCAR's Community Climate System Model (CCSM), one of the IPCC models that loses sea ice year-round at this CO₂ concentration. A new method is developed to disable the convective cloud feedback in the Community Atmosphere Model (CAM), the atmospheric component of CCSM, and to show that March sea ice cannot be eliminated in CCSM at CO₂ = 1120 ppm without the aid of the convective cloud feedback.

1. Introduction

Sea ice plays a crucial role in Arctic climate, particularly during winter, when it insulates the atmosphere from the relatively warm ocean. This allows the atmosphere to drop to extremely low temperatures during

polar night, which can affect lower latitudes when cold fronts of Arctic air penetrate southward. Significant loss of sea ice would put immediate strain on Arctic biota (Smetacek and Nicol 2005), could accelerate the melting of the Greenland ice sheet (Lemke et al. 2007), and could affect global climate by causing changes in atmospheric and oceanic circulation (Serreze et al. 2007; McBean et al. 2005). Furthermore, because ice-free conditions in the Arctic would allow increased shipping and exploitation of natural resources, an accurate assessment

Corresponding author address: Dorian Abbot, EPS Department, Harvard University, 20 Oxford St., Cambridge, MA 02138.
E-mail: abbot@fas.harvard.edu

of the probability of such conditions is extremely important for the economic futures of the nations surrounding the Arctic.

The state-of-the-art coupled ocean–sea ice–land–atmosphere global climate models (GCMs) that participated in the Intergovernmental Panel on Climate Change (IPCC) Fourth Assessment Report (AR4) show a vast divergence in winter sea ice forecasts at a CO_2 of 1120 ppm. In fact, the spread in forecasts among the models is so large that two of them [the National Center for Atmospheric Research (NCAR) Community Climate System Model, version 3.0 (CCSM3.0) and Max Planck Institute (MPI) ECHAM5] lose nearly all winter sea ice (Winton 2006), and some others yield very little change in winter sea ice at all. Given that the IPCC models are generally taken to represent the highest embodiment of our understanding of the climate system, the fact that they produce such a high spread in their forecast of an important climate variable is both interesting and disturbing.

Although a CO_2 concentration of 1120 ppm is high, it is not beyond the realm of possibility. In fact, known fossil fuel reserves ensure that with just a little “drill, baby, drill” spirit, humanity can increase the CO_2 concentration to 2000 ppm over the next 100–200 yr (Archer and Brovkin 2008). Additionally, there is reason to believe that the two models that lose sea ice year-round at $\text{CO}_2 = 1120$ ppm are at least as reliable as the other models. For example, CCSM has a sophisticated sea ice model (Briegleb et al. 2004) that produces one of the better simulations of current sea ice loss in the Arctic among IPCC models (Stroeve et al. 2007). Therefore, we should consider it possible that the Arctic will be sea ice-free throughout the year within the next few hundred years.

Given the climatic and economic importance of winter sea ice and the uncertainty of forecasts made using our best forecasting tools, it is important to try to understand the feedbacks that might play a role in creating this uncertainty. Various positive feedback mechanisms have been identified that could enhance changes in sea ice as the polar climate warms. For example, increases in solar absorption as sea ice recedes could lead to surface heating and further reductions in sea ice (ice–albedo feedback; see Budyko 1969; Sellers 1969). Similarly, increases in ocean heat transport (OHT) can be a major contributor to sea ice loss (e.g., Holland et al. 2006; Winton 2006), and sea ice loss may increase ocean heat transport (Bitz et al. 2006; Holland et al. 2006), which closes a feedback loop. Changes in clouds could also represent an important feedback, because clouds make a significant contribution to atmospheric optical depth in the Arctic (Intrieri et al. 2002a,b), which is important for

predicting sea ice extent (Francis et al. 2005). Changes in Arctic clouds may be particularly important during winter (Vavrus et al. 2008), when they may play a critical role in polar amplification (Holland and Bitz 2003).

A winter convective cloud feedback that may strongly affect Arctic winter sea ice at increased atmospheric CO_2 concentrations has recently been proposed and investigated in the context of explaining equable climates, for example, the climate of the Eocene (Abbot and Tziperman 2008a,b, 2009; Abbot et al. 2009). This feedback is initiated by CO_2 -induced warming, which leads to some sea ice loss. This allows increased heat and moisture fluxes from the ocean surface, which, in turn, leads to atmospheric convection, and to the development of optically thick tropospheric convective clouds and increased high-altitude moisture. These clouds and moisture trap outgoing longwave radiation and therefore result in further warming and sea ice loss in the Arctic. A related suggestion of such a feedback was also briefly made by Sloan et al. (1999) and Huber and Sloan (1999). Additionally, a number of authors have discussed the potential for a nonconvective polar stratospheric cloud feedback (Sloan et al. 1992; Sloan and Pollard 1998; Peters and Sloan 2000; Kirk-Davidoff et al. 2002; Kirk-Davidoff and Lamarque 2008).

The convective cloud feedback should occur preferentially during winter for two reasons. First, during polar night the atmosphere cools much quicker than the ocean, because the ocean has a much higher heat capacity than the atmosphere. This causes heat and moisture fluxes from the ocean to the lower atmosphere, significantly destabilizing the atmosphere. Second, during summer low-level clouds block low-level atmospheric absorption of solar radiation so that atmospheric absorption of solar radiation occurs preferentially in the midtroposphere and stabilizes the lower atmosphere to convection. Because the incoming solar radiation is either small or absent at high latitudes during winter, when the feedback should be most active, the cloud albedo is irrelevant and any clouds the mechanism produces lead to warming. Our hypothesis is that at increased CO_2 levels the convective cloud feedback will produce a positive forcing on the high-latitude energy balance that can help the Arctic to remain ice free throughout polar night. By increasing sea surface temperatures during winter, the feedback should also help to reduce the formation of sea ice, so that the sea ice concentration will be lower in late winter, when sea ice reaches its seasonal maximum.

The focus of this paper is to determine whether this convective cloud feedback plays an important role in the reduction or elimination of Arctic sea ice during winter at high CO_2 levels in climate models. We restrict the

scope of this work to the investigation of models because the atmospheric CO₂ concentration required to cause large reductions in winter sea ice is far beyond the current CO₂ level.

In section 2 we investigate archived output from the GCMs that participated in the Intergovernmental Panel on Climate Change Fourth Assessment Report scenario prescribing a 1% yr⁻¹ CO₂ increase until the CO₂ is 4 times higher (1120 ppm) than its preindustrial value (280 ppm), which we will refer to as IPCC AR4 4 × CO₂. A comparison of these models motivates the suggestion that the convective cloud feedback might play an important role in reducing late-winter sea ice in the models that lose it. In section 3 we perform a sensitivity analysis comparing the importance of the ocean heat transport feedback to that of the convective cloud feedback in eliminating maximum seasonal (late winter) sea ice in NCAR's coupled CCSM model. We do this using the Community Atmosphere Model (CAM), the atmospheric component of CCSM, coupled to a mixed layer ocean and thermodynamic sea ice model. In section 4 we discuss the implications and caveats of this work, and in section 5 we review our central conclusions. We describe in detail our method of disabling the ocean heat transport and convective cloud feedbacks in CAM in the appendix.

2. The convective cloud feedback in the IPCC coupled GCM archive

In this section we show that the convective cloud feedback is active during winter in the state-of-the-art coupled ocean–sea ice–land–atmosphere GCMs of the IPCC AR4 4 × CO₂ scenario that lose some or all of the winter sea ice. We then suggest that the feedback may be important for determining the late-winter sea ice predictions of these models. We will focus in particular on the region over the ocean and north of 80°N, which we will refer to as the “polar” region. This choice of region accentuates change in winter sea ice because it is covered in sea ice in all models at the beginning of the experiment, when the CO₂ concentration is 280 ppm.

We obtained the IPCC model output from the World Climate Research Programme's (WCRP's) Coupled Model Intercomparison Project phase 3 (CMIP3) multimodel dataset. Each modeling center does not necessarily supply all model output that the CMIP3 archive requests for each emission scenario. In cases in which there was missing output, we requested it directly from the appropriate modeling center. We omit the models for which we were not able to acquire missing output from any plot for which that output is necessary.

There is a marked difference between the winter Arctic climate of models that lose winter sea ice and those

that retain it. Figure 1 demonstrates this by showing the change in Arctic winter climate over the experiment for a model that lost nearly all winter sea ice (NCAR CCSM3.0) and a model that showed relatively little change in winter sea ice [Geophysical Fluid Dynamics Laboratory Climate Model version 2.0 (GFDL CM2.0)]. Associated with the Arctic-wide loss of winter sea ice in the NCAR model (Fig. 1a) is a warming of the surface air temperature by up to 25°–30°C (Fig. 1b). This change in temperature is forced in part by a strong increase in cloud radiative forcing (CRF; the difference between the net radiative flux at the top of the atmosphere in all-sky and clear-sky conditions) over the Arctic (Fig. 1c), which extends throughout regions of the Arctic where there is a large change in sea ice. There is a major increase in the convective precipitation rate throughout the Arctic in the NCAR model (Fig. 1d), implying that the increase in CRF is associated with the onset of convection and convective clouds (convective precipitation is the best available indicator of convection archived in the CMIP3 dataset).

In contrast, the GFDL model shows very little change in winter sea ice over the polar region (Fig. 1e) and has only roughly half the surface air temperature warming (Fig. 1f) as that of the NCAR model (Fig. 1b). There is no change in CRF (Fig. 1g) and no change in convective precipitation (Fig. 1h) in the polar region in this model; however, there is a large change in winter sea ice between Scandinavia and Svalbard (70°–80°N latitude). Associated with this local change in sea ice is a change in surface air temperature that is much larger than that in surrounding areas (Fig. 1f), a strong increase in CRF (Fig. 1g), and a large change in convective precipitation (Fig. 1h). Even though there are not increases in CRF associated with convective clouds over the pole in the GFDL model, local increases in CRF in the GFDL model in the regions where the GFDL model loses winter sea ice are as large as Arctic-wide increases in CRF in the NCAR model.

Winter convection should cause a rearrangement in the vertical profile of winter clouds in regions that have lost winter sea ice. We see just such a rearrangement in the polar region of the NCAR model over the course of the IPCC AR4 4 × CO₂ scenario run, where the cloud fraction increases significantly during the winter in the altitude range from roughly 600 to 900 mb, but it decreases below 900 mb (Fig. 2a). Given the increase in convective precipitation (Fig. 1d) and the single-column model results of Abbot and Tziperman (2008b), we interpret this change in the cloud's vertical structure as being caused by low-level convection. We will show conclusively that this is the case in CAM, the atmospheric component of CCSM, in section 3. During summer, changes in cloud fraction in the NCAR model are not

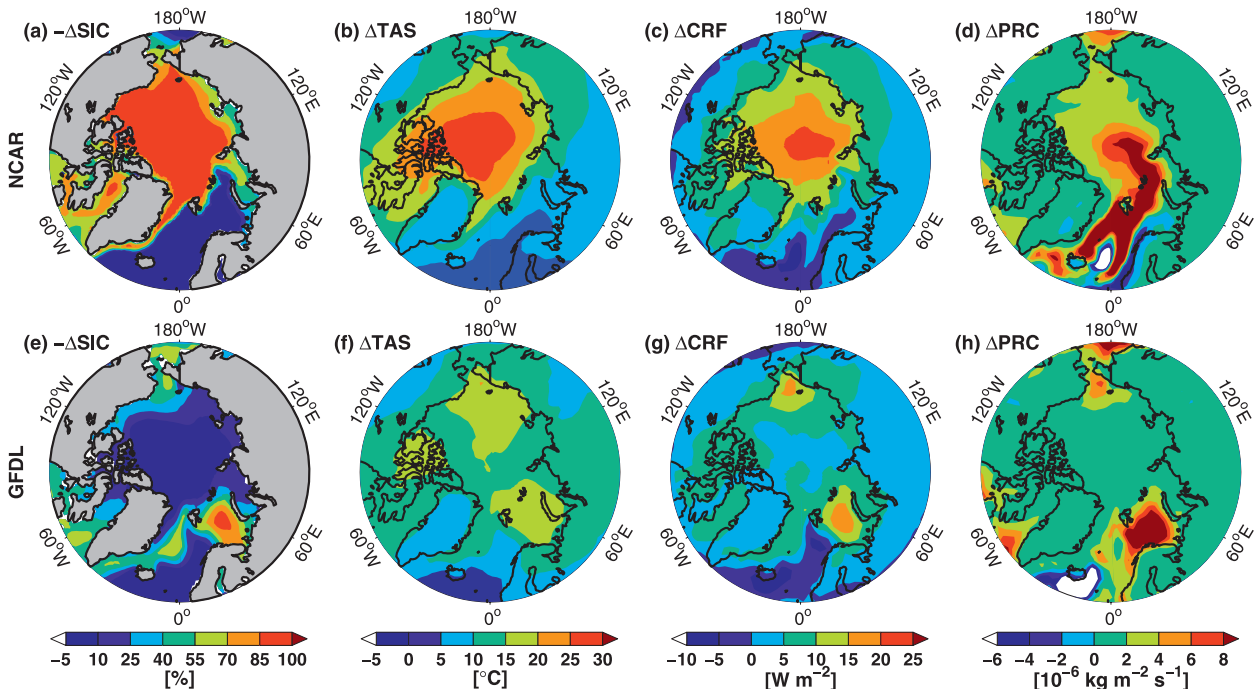


FIG. 1. Change in winter (November–February) Arctic climate over the course of the IPCCAR4 $4 \times \text{CO}_2$ experiment. The models are (a)–(d) NCAR CCSM3.0, which loses most Arctic winter sea ice and (e)–(h) GFDL CM2.0, which loses minimal winter Arctic winter sea ice. For each variable, the difference between the mean over the last 10 yr and the mean over the first 10 yr is plotted. (a),(e) $-\Delta\text{SIC}$, the negative of the change in sea ice concentration (100% means a complete loss of sea ice); (b),(f) ΔTAS , the change in surface air temperature; (c),(g) ΔCRF , the change in cloud radiative forcing; and (d),(h) ΔPRC , the change in convective precipitation rate.

consistent with the low-level decrease and higher-level increase that would indicate increased convection. The situation is quite different in the GFDL model, in which there is no convection during winter and the winter polar cloud fraction decreases (Fig. 2b). Interestingly, the change in cloud profile in the GFDL model during the month of October does suggest the onset of convection over the IPCC AR44 $\times \text{CO}_2$ scenario run. Additionally, there are large increases in convective precipitation and cloud radiative forcing in the GFDL model during this month (not shown). The GFDL model loses sea ice throughout the Arctic by the end of the run during the month of September, but has regained much of the sea ice coverage by November (not shown). In the transition month of October the convective signal that is present in the NCAR model is present in the GFDL model, but sea ice quickly reforms in the GFDL model and the convection ceases.

In Fig. 3a we plot the November–February cloud radiative forcing at $\text{CO}_2 = 1120$ ppm in all the IPCC models from the CMIP3 archive as a function of the November–February sea ice volume in the polar region (see Fig. 4 for model symbol legend). Based on the line of best fit, the average winter CRF is about 14 W m^{-2} higher in the models that completely lose winter polar

sea ice at quadrupled CO_2 than in the models with the largest amount of sea ice remaining. As a point of comparison, a doubling of CO_2 leads to a global mean radiative forcing of only 3.7 W m^{-2} (Forster et al. 2007). Additionally, the MPI model loses an average of 39 W m^{-2} from the surface between November and February and the NCAR model loses 54 W m^{-2} , so that this additional CRF is a significant term in the high-latitude winter heat balance. This implies that the degree of activity of the convective cloud feedback, which can provide a strong radiative warming throughout the winter, could be important for determining the late-winter sea ice in these models. Indeed, there does appear to be some relation between the activity of the convective cloud feedback during winter and the decrease in March polar sea ice volume in the IPCC models (Fig. 3b). The relation between changes in winter cloud radiative forcing and March sea ice, however, may indicate nothing more than the fact that models that lose more winter sea ice are likely to lose more March sea ice. In any case, we view the relation between changes in winter cloud radiative forcing and changes in March sea ice in the IPCC models as a reasonable basis for a working hypothesis that the convective cloud feedback could be important for predicting late-winter sea ice at

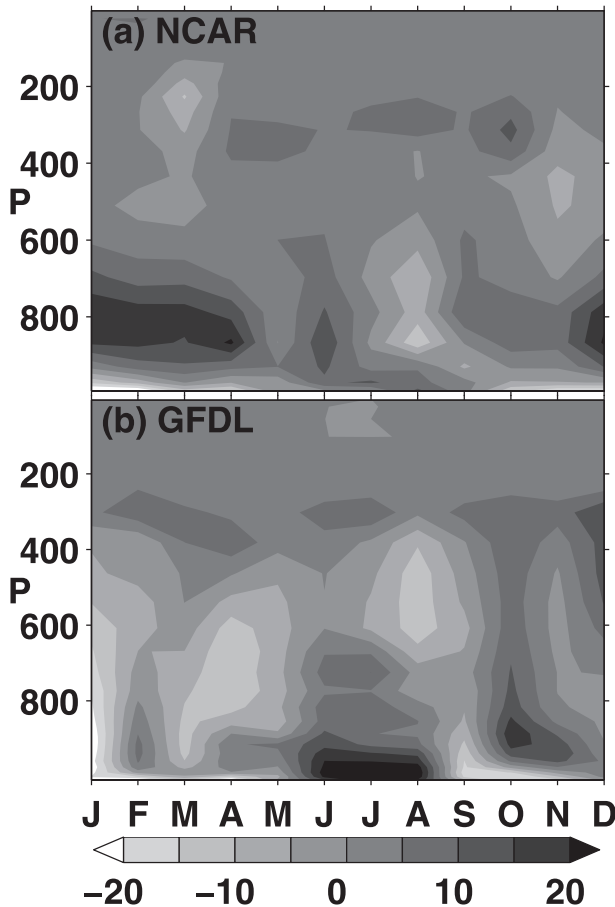


FIG. 2. Change in the seasonal cycle of polar cloud fraction for the (a) NCAR CCSM3.0 and (b) GFDL CM2.0 models over the course of the IPCC AR4 \times CO₂ scenario run. The change in polar cloud fraction is defined as the difference between the mean cloud fraction over the last 10 yr and the mean over the first 10 yr and is plotted as a function of month and elevation. Convection-induced changes are evident during the winter in the NCAR model.

high greenhouse gas levels, and we will investigate this hypothesis in more detail in section 3.

3. Importance of the convective cloud feedback for March sea ice reduction in CCSM

NCAR's coupled ocean-atmosphere model (CCSM) is one of the models from the IPCC archive analyzed in section 2 that lost most of its winter sea ice over the course of the AR4 \times CO₂ scenario. In this section we use NCAR's CAM, the atmospheric component of CCSM, to determine more firmly whether the convective cloud feedback plays an important role in the loss of winter sea ice at CO₂ = 1120 ppm in this model. We run CAM at T42 resolution coupled to a mixed layer with a constant depth of 50 m and specified ocean heat transport. We focus on comparing the convective cloud

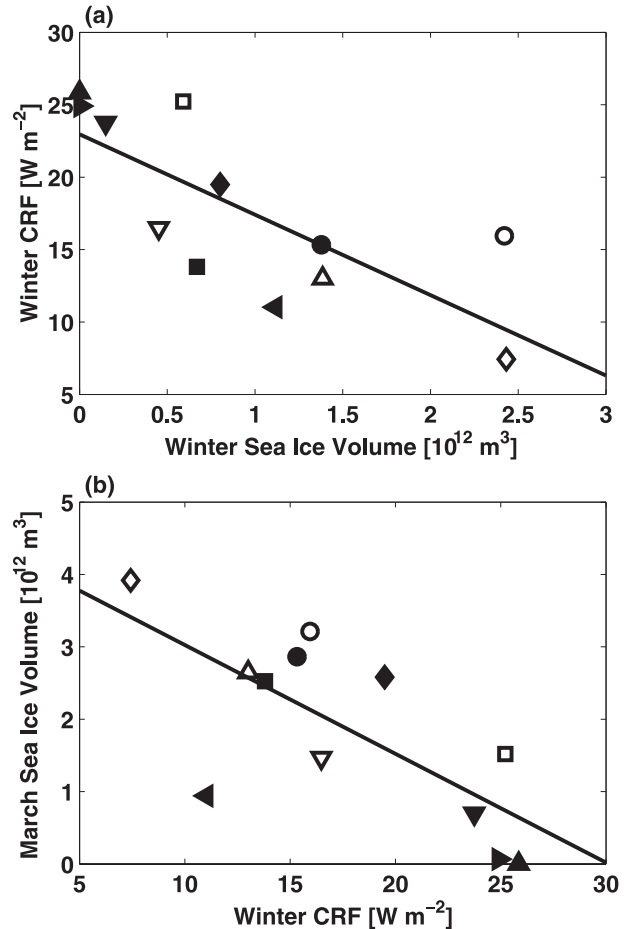


FIG. 3. Evidence that changes in cloud radiative forcing are associated with changes in sea ice in the Arctic during winter in the IPCC coupled GCMs at quadrupled CO₂ (1120 ppm). (a) Winter (November–February) polar (sea north of 80°N) CRF as a function of winter polar sea ice volume ($r^2 = 0.57$, $p = 0.004$). (b) March sea ice volume as a function of winter cloud radiative forcing ($r^2 = 0.52$, $p = 0.008$). Plotted results are obtained by averaging the output from the models over the last 10 yr of runs from the IPCC AR4 \times CO₂ scenario. See Fig. 4 for model symbol legend.

feedback with the ocean heat transport feedback, that is, the increase of ocean heat transport into the Arctic associated with increasing CO₂ that may be caused by the reduction in sea ice itself. Changes in ocean heat transport have previously been identified as an important component of high-CO₂ sea ice loss in CCSM (e.g., Holland et al. 2006; Winton 2006). We find that both feedbacks must be active for year-round elimination sea ice to occur in the Arctic at a CO₂ concentration of 1120 ppm in this model. As we will discuss in section 4, there are many other feedbacks that may be important for determining sea ice that we do not consider here.

To measure the comparative strengths of the ocean heat transport feedback and convective cloud feedback,

○	CCMA CGCM3.1
□	CNRM CM3
◇	GFDL CM2.0
△	GFDL CM2.1
◁	GISS
▷	INGV ECHAM4
▽	INMCM3.0
●	IPSL CM4
■	MIROC3.2 MEDRES
◆	MIUB ECHO
▲	MPI ECHAM5
◀	MRI CGCM2.3.2a
▶	NCAR CCSM3.0
▼	UKMO HADGEM1

FIG. 4. Symbols used to denote the IPCC models in Fig. 3.

we run CAM at a CO_2 concentration of 1120 ppm in the following four configurations: 1) with both feedbacks turned off (LO OHT, LO CRF), 2) with only the convective cloud feedback on (LO OHT, HI CRF), 3) with only the ocean heat transport feedback on (HI OHT, LO CRF), and 4) with both feedbacks on (HI OHT, HI CRF). We turn a feedback off in CAM by forcing the appropriate variable to its preindustrial ($\text{CO}_2 = 280$ ppm) value from the CCSM IPCC AR4 $4 \times \text{CO}_2$ run, and we turn a feedback on by forcing the appropriate variable to its $\text{CO}_2 = 1120$ ppm value from the CCSM IPCC AR4 $4 \times \text{CO}_2$ run. See the appendix for details of this methodology.

Figure 5 shows the change in heating caused by turning the convective cloud feedback and ocean heat transport feedback on. The difference in radiative forcing caused by the onset of the convective cloud feedback (Fig. 5a) is broad, positive, and nearly zonally symmetric throughout the Arctic. The change in ocean heat transport convergence during the winter caused by the onset of the ocean heat transport feedback (Fig. 5b) shows much smaller-scale structure, is generally of a smaller magnitude, and is negative in some places. A major change in ocean heat transport occurs, with the ocean heat transport convergence decreasing significantly in the North Atlantic and increasing in the deep Arctic. This reflects the fact that some of the heat deposited in the North Atlantic in

the LO OHT case is instead deposited in the deep Arctic in the HI OHT case, as would be expected if an OHT feedback on sea ice loss were operating in the model.

From Fig. 5, the changes in cloud radiative forcing appear to be much stronger than the changes in ocean heat transport. For example, the feedback parameter for polar winter cloud radiative forcing, the change in polar winter cloud radiative forcing per degree of global mean temperature change, is $4.4 \text{ W m}^{-2} \text{ K}^{-1}$, while the feedback parameter for polar winter ocean heat transport is $1.2 \text{ W m}^{-2} \text{ K}^{-1}$. Heat delivered to the bottom of sea ice, however, may be more effective at preventing winter sea ice growth than heat delivered to the top. This is because ice growth occurs at the ice bottom, so that changes in heat flux at the ice bottom have a direct effect on ice growth, whereas changes in heat flux at the ice surface must diffuse through the ice to affect ice growth (Eisenman et al. 2009).

To establish that the increase in cloud radiative forcing in CAM is due to the convective cloud feedback, rather than changes in clouds forced by changes in large-scale circulation, we show the seasonal cycle of the moist convective mass flux in the model configurations used in the LO CRF and HI CRF runs (Fig. 6). There is a clear increase in atmospheric convection during winter in the HI CRF case (Fig. 6b), which mirrors the increase in cloud fraction over the course of the CCSM run from section 2 (Fig. 2a).

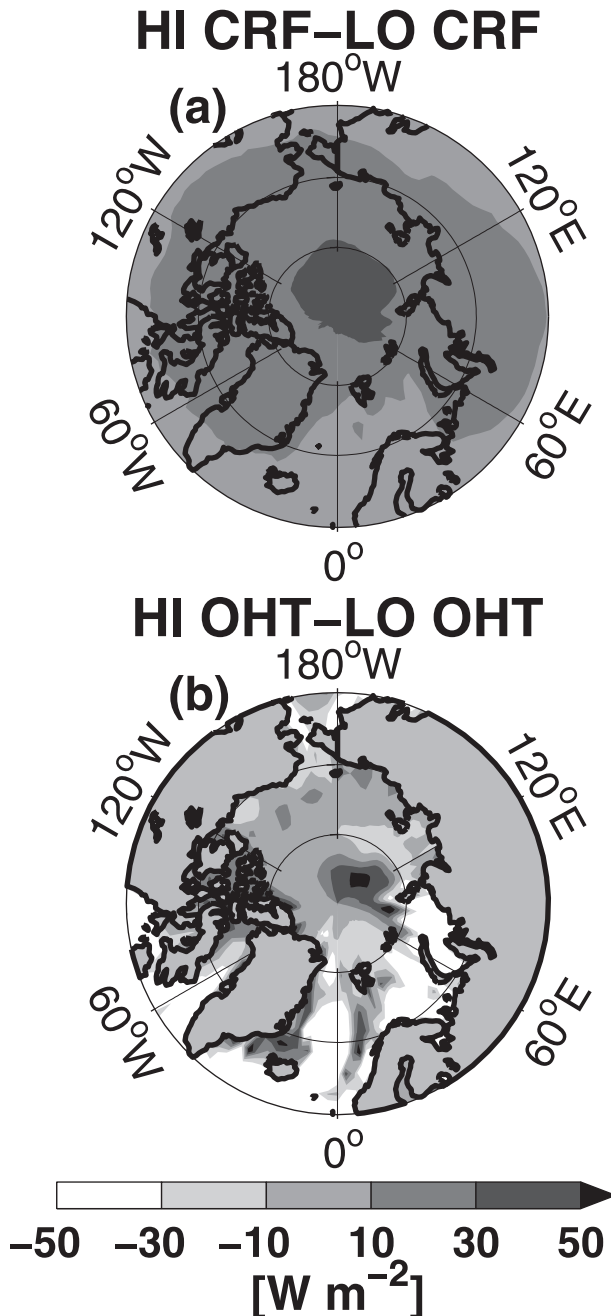


FIG. 5. Comparison of the strengths of the convective cloud feedback and OHT feedback during winter. (a) Cloud radiative forcing averaged between November and February in the HI CRF case minus the LO CRF case (change in CRF between the two cases). (b) Ocean heat transport convergence averaged between November and February in the HI OHT case minus the LO OHT case (change in OHT convergence between the two cases). See text for details.

When we run CAM with the CO_2 increased to 1120 ppm and both feedbacks turned off (LO OHT, LO CRF), the Arctic ocean is largely covered with sea ice during March (Fig. 7a) that has a thickness of between 0.8 and 1.6 m in most regions (Fig. 7e) for a total Northern Hemisphere sea ice volume of $14 \times 10^{12} \text{ m}^3$. When the convective cloud feedback alone is turned on (LO OHT, HI CRF), there is a slight reduction in the March sea ice extent (Fig. 7b), and the sea ice thickness is generally less than 1.2 m (Fig. 7f), so that the total Northern Hemisphere sea ice volume is $8.0 \times 10^{12} \text{ m}^3$. When we turn only the ocean heat transport feedback on (HI OHT, LO CRF), a somewhat larger reduction in March sea ice (Figs. 7c,g, total sea ice volume of $3.9 \times 10^{12} \text{ m}^3$) results than when the convective cloud feedback alone is active; however, the important result is that both feedbacks are necessary (HI OHT, HI CRF) for a near-complete removal of March sea ice (Figs. 7d,h, total sea ice volume of $0.51 \times 10^{12} \text{ m}^3$).

4. Discussion

The March polar sea ice volume forecasts by the model runs of the IPCC AR4 $4 \times \text{CO}_2$ scenario (section 2) are entirely uncorrelated with the models' equilibrium $2 \times \text{CO}_2$ climate sensitivity (equilibrium change in global mean surface temperature when CO_2 is doubled, see Fig. 8a), their transient $2 \times \text{CO}_2$ climate sensitivity (change in global mean surface temperature at the time of CO_2 doubling in a $1\% \text{ yr}^{-1}$ CO_2 increase experiment, see Fig. 8b), and semiequilibrium $4 \times \text{CO}_2$ climate sensitivity (the change in global mean surface air temperature over the course of the IPCC AR4 $4 \times \text{CO}_2$ experiment, which allows ~ 160 yr of equilibration after the CO_2 reaches 1120 ppm; see Fig. 8c).

These important results indicate that the conventional measures of sensitivity to global climate change are not useful for predicting the critical climate phenomenon of March Arctic sea ice loss: "more sensitive" models are no more likely to lose March Arctic sea ice than "less sensitive" models. This may be in part because global sensitivity measures cannot predict which model will be most affected by the convective cloud feedback and other Arctic-specific feedbacks, which may lead to "tipping point behavior" (Winton 2006; Eisenman and Wettlauffer 2009; Winton 2008; Stern et al. 2008). Previous work has also shown that Arctic sea ice simulation and prediction are uncertain because of additional cloud-related complications (Eisenman et al. 2007; Eisenman 2007).

Only two models show a complete collapse of winter sea ice in the IPCC AR4 $4 \times \text{CO}_2$ scenario (section 2): the MPI model (after roughly one CO_2 doubling) and the NCAR model [during the equilibration time after

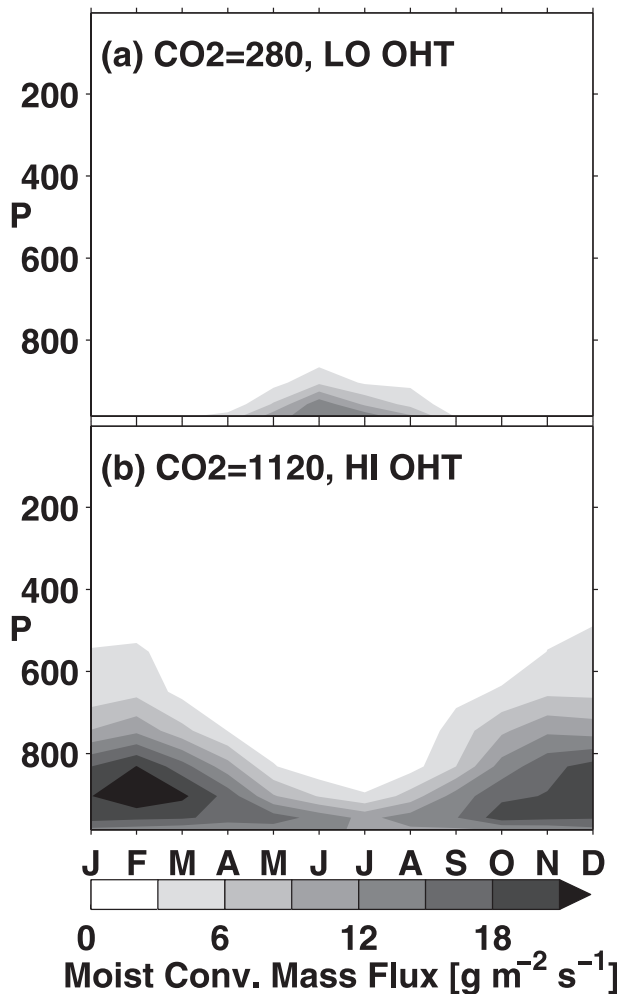


FIG. 6. Seasonal cycle in moist convective mass flux (month vs vertical level) averaged over the polar region in CAM when it is run with a 50-m mixed layer and interactive clouds in the following configurations: (a) a CO_2 concentration of 280 ppm and “LO OHT” (which reproduces the climate in CCSM at the start of the IPCC AR4 $4 \times \text{CO}_2$ run) and (b) a CO_2 concentration of 1120 ppm and “HI OHT” (which reproduces the climate in CCSM at the end of the IPCC AR4 $4 \times \text{CO}_2$ run). See the appendix for details. Strong winter convection over the Arctic in the $\text{CO}_2 = 1120$ ppm, HI OHT run is evident.

the second CO_2 doubling (Winton 2006)]; however, the convective cloud feedback is still relevant for the other models and possibly for future climate. The change in winter polar cloud radiative forcing in all participating models increases roughly linearly with the decrease in winter sea ice volume (Fig. 3a). This suggests that the convective cloud feedback is present, but not fully active, even in models that do not completely lose winter sea ice. This, in turn, suggests that all of the models would show a more dramatic increase in winter cloud radiative forcing, similar to that in the NCAR and MPI

models, if the CO_2 were further increased or the integration were continued until the models were fully equilibrated.

The activation of the convective cloud feedback in a coupled GCM is the result of a combination of many different, complex, and uncertain parameterizations and parameters, including those in the sea ice, radiation, convection, and cloud schemes. It is therefore not possible to identify a single reason indicating that two models (NCAR and MPI) show this feedback fully active and completely lose sea ice at quadrupled CO_2 , whereas the feedback is only partially active or not active at all in other models. Because it seems likely that the feedback would activate in all of the IPCC models if the CO_2 were further increased, the disagreement between these state-of-the-art models appears to reflect uncertainty in the threshold CO_2 at which the feedback activates (see also Abbot and Tziperman 2009).

Observational evidence suggests that during fall sea ice loss is associated with increased cloud height and deepening of the boundary layer (Schweiger et al. 2008), which could be due to increased convection. We are currently investigating the convective cloud feedback using the observational record to determine, for example, whether anomalies in sea ice during winter are related to anomalies in clouds, convection, and cloud radiative forcing. Comparing these quantitative results to model output should allow us to determine which models reproduce the convective cloud feedback best. This may help us understand the large spread in winter sea ice forecasts in the IPCC AR4 $4 \times \text{CO}_2$ experiment (section 2) and potentially might allow insight into which model results are most realistic.

Both the convective cloud and ocean heat transport feedbacks must be active in order to eliminate March sea ice at $\text{CO}_2 = 1120$ ppm in CCSM (section 3). Because the HI CRF forcing field is generated using output derived from CCSM once sea ice has been completely eliminated, the HI CRF forcing field implicitly depends on the ocean heat transport feedback, which was also necessary to eliminate sea ice. Similarly, the HI OHT forcing field depends on the convective cloud feedback, which helped to eliminate sea ice in the CCSM run and change the ocean heat transport. Therefore, in some sense, our methodology of section 3 does not fully separate the two feedbacks in the LO OHT, HI CRF case and the HI OHT, LO CRF cases. That said, our main conclusion from section 3—that the elimination of March sea ice in CCSM at $\text{CO}_2 = 1120$ ppm requires both feedbacks—remains valid.

Although many feedbacks may be important for determining winter sea ice, in section 3 we only compared the strength of the convective cloud feedback with that

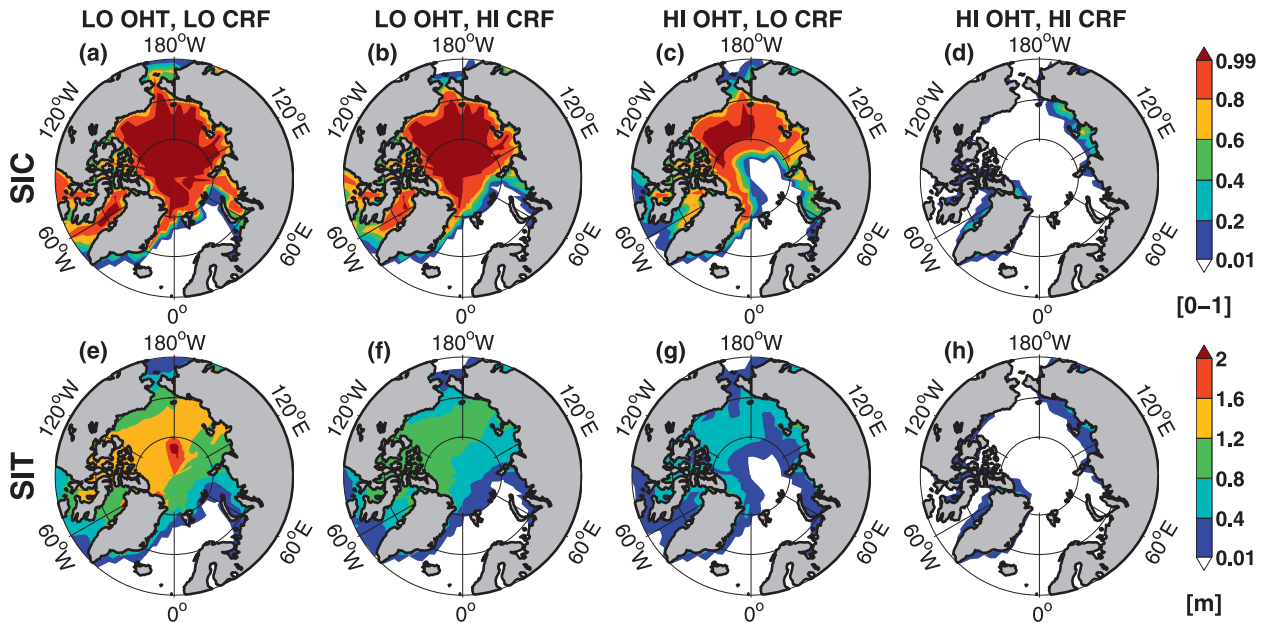


FIG. 7. March (a)–(d) sea ice concentration (SIC) and (e)–(h) sea ice thickness in CAM when it is run with a 50-m mixed layer depth at a CO_2 concentration of 1120 ppm and (a), (e) the OHT and convective cloud (CC) feedbacks both off (LO OHT, LO CRF), (b), (f) the OHT feedback off and the CC feedback on (LO OHT, HI CRF), (c), (g) the OHT feedback on and the CC feedback off (HI OHT, LO CRF), and (d), (h) both feedbacks on (HI OHT, HI CRF). Both feedbacks must be active for the complete removal of March sea ice. See text for details.

of the ocean heat transport feedback in CAM. A feedback we did not consider, because we fixed the mixed layer depth to 50 m globally, is the mixed layer depth feedback, which may have an important effect on winter sea ice (Ridley et al. 2007). This feedback describes the deepening of the ocean mixed layer during winter, when sea ice is removed, which allows the ocean to stay warm longer during winter and makes sea ice less likely to form. The fact that March sea ice was eliminated in CAM in the HI OHT, HI CRF case even with this feedback disabled indicates that the mixed layer depth feedback is not as important in this model as the convective cloud and ocean heat transport feedbacks, both of which are necessary for the elimination of March sea ice in CAM.

We also did not explicitly consider the ice–albedo feedback, which might be important for determining intermodel spread in March sea ice forecasts (Eisenman and Wettlaufer 2009). Because we did not disable the sea ice–albedo feedback in our CAM runs (section 3), this feedback may play some role in causing the differences between the March sea ice predictions in our four model configurations. For example, there is more summer sea ice in the LO OHT, HI CRF case than in the HI OHT, LO CRF case, which means less solar radiation is absorbed in the LO OHT, HI CRF case than in the HI OHT, LO CRF case. Consequently, some of the re-

duction in March sea ice in the run with the ocean heat transport feedback alone relative to the run with the convective cloud feedbacks alone may be due to summer sea ice reflecting more solar radiation in the latter run. The convective cloud feedback must be, in some sense, “weaker” than the ocean heat transport feedback, but the sea ice–albedo feedback exaggerates this difference in strength to create a larger difference in March sea ice than would exist if the albedo were fixed to be the same in both sensitivity configurations. In any case, the central conclusion of section 3—that both the ocean heat transport feedback and the convective cloud feedback are necessary for the nearly complete removal of March sea ice in CCSM when the CO_2 is increased to 1120 ppm—remains valid.

Finally, there has been substantial debate about whether increases in atmospheric latent heat transport resulting from increased temperature can overcome decreases in eddy activity and lead to increases in atmospheric heat transport as the climate warms (Pierrehumbert 2002; Caballero and Langen 2005; Solomon 2006; Graverson et al. 2008). Although an increase in atmospheric heat transport resulting from latent heat transport would not necessarily be caused directly by sea ice loss, so it would not necessarily represent a positive feedback, such a change could affect sea ice concentration. This means that some of the intermodel spread in sea ice forecast

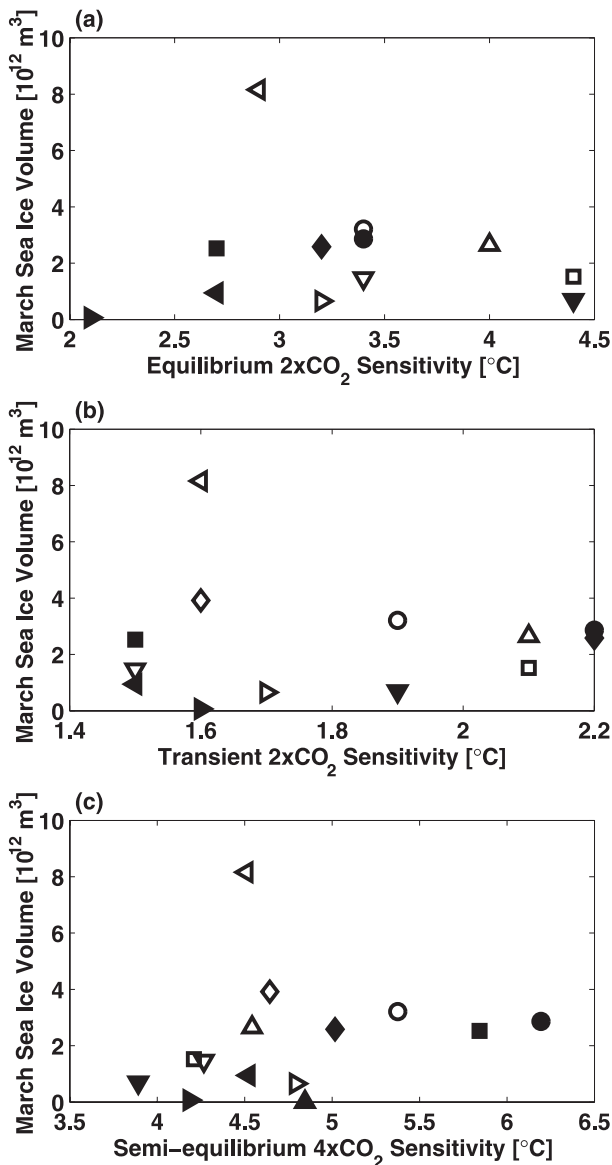


FIG. 8. Lack of correlation between March polar sea ice forecasts at $\text{CO}_2 = 1120$ ppm and global climate sensitivity. Change in March polar sea ice volume as a function of (a) equilibrium $2 \times \text{CO}_2$ climate sensitivity (equilibrium change in global mean surface temperature when CO_2 is doubled, $r^2 = 0.005$), (b) the transient $2 \times \text{CO}_2$ climate sensitivity (change in global mean surface temperature at the time of CO_2 doubling in a $1\% \text{ yr}^{-1}$ CO_2 increase experiment, $r^2 = 0.0005$), and (c) semiequilibrium $4 \times \text{CO}_2$ climate sensitivity (the change in global mean surface air temperature over the course of the IPCC AR4 $4 \times \text{CO}_2$ experiment, which allows ~ 160 yr of equilibration after the CO_2 reaches 1120 ppm, $r^2 = 0.04$). See Fig. 4 for model symbol legend.

could be due to differences in the simulation of atmospheric heat transport simulation.

The convective cloud feedback should lead to increases in high-altitude moisture that would produce

additional effects on radiative transfer above those caused by the onset of optically thick convective clouds. In the sensitivity analysis of section 3, we only included changes in cloud radiative forcing in our specification of the convective cloud feedback, so we ignored any effects on radiative transfer that convection-induced changes in moisture might have. This could lead to an underestimation of the effects of the convective cloud feedback; however, we have performed experiments with NCAR's single-column atmosphere model (SCAM) that suggest that neglecting changes in moisture reduces the radiative strength of the convective cloud feedback by only about 10%–20%.

5. Conclusions

In this paper we investigated the effect of a convective cloud feedback on winter sea ice at high CO_2 concentrations. In this feedback, CO_2 -initiated warming leads to sea ice reduction, which allows increased heat and moisture fluxes from the ocean surface. This destabilizes the atmosphere and leads to atmospheric convection. The atmospheric convection produces optically thick convective clouds and increases high-altitude moisture levels, both of which trap outgoing longwave radiation and therefore result in further warming and sea ice loss. We summarize our main findings and conclusions as follows.

- The convective cloud feedback (Abbot and Tziperman 2008a,b, 2009) is active during the winter (November–February) at a CO_2 concentration of 1120 ppm in the IPCC coupled global climate models that lose most Arctic winter sea ice.
- At $\text{CO}_2 = 1120$ ppm, IPCC model forecasts of maximum seasonal (March) sea ice volume are correlated with polar winter cloud radiative forcing, which the convective cloud feedback increases, whereas they are entirely uncorrelated with model global climate sensitivity.
- Both the convective cloud feedback and the ocean heat transport feedback (e.g., Bitz et al. 2006; Holland et al. 2006; Winton 2006) are necessary to eliminate the March sea ice at $\text{CO}_2 = 1120$ ppm in NCAR's CCSM, one of two coupled IPCC models that lost nearly all March sea ice. If either feedback is disabled, March sea ice remains.

Acknowledgments. We thank Brian Farrell, Peter Huybers, Zhiming Kuang, Dan Schrag, and three anonymous reviewers for comments. We thank Ian Eisenman especially for his extensive help and comments. We thank Rodrigo Caballero and Peter Langen for technical

advice. We acknowledge the international modeling groups, the Program for Climate Model Diagnosis and Intercomparison (PCMDI), and the WCRP's Working Group on Coupled Modelling (WGCM) for their roles in making the WCRP CMIP3 multimodel dataset available. Support of this dataset is provided by the Office of Science, U.S. Department of Energy. DA was supported by an NSF graduate research fellowship for part of the time during which this work was completed. This work is funded by the NSF paleoclimate program, ATM-0455470, and the McDonnell Foundation.

APPENDIX

Method of Turning Feedbacks On and Off

Below we describe in detail the way in which we force the ocean heat transport and cloud radiative forcing to specified values in NCAR's Community Atmosphere Model (CAM) for the sensitivity analysis performed in section 3. We run CAM in slab ocean mode with a fixed ocean mixed layer depth of 50 m everywhere. In each case we run CAM until it reaches a statistically equilibrated seasonal cycle (30–50 yr) and then average all quantities over 10 subsequent years of output.

a. Ocean heat transport feedback

Ocean heat transport convergence, sometimes called “qflux,” must be specified to CAM at each grid point for each month. We calculate the qflux that we specify to CAM based on output from the NCAR CCSM run from the IPCC AR4 $4 \times \text{CO}_2$ scenario. CCSM is a fully coupled model that dynamically calculates ocean heat transport. We do this using the code “defineqflux.c,” which is distributed with CAM. This code calculates the qflux from the surface heat balance

$$\rho_w C_p D \Delta(\text{SST}) = \text{SW} - \text{LW} - \text{LH} - \text{SH} \\ - \text{QFLUX} + \rho_i L_i \Delta h_i,$$

where ρ_w is the density of water, C_p is the heat capacity of water, D is the mixed layer depth, $\Delta(\text{SST})$ is the change in sea surface temperature over the month, SW is the net downward shortwave radiation flux at the surface, LW is the net upward longwave radiation at the surface, LH is the latent heat flux, SH is the sensible heat flux, ρ_i is the density of ice, L_i is the heat of fusion of ice, and Δh_i is the change in average ice thickness in the grid box. Because the output of the CCSM run provides every variable in the above equation except QFLUX, we can use this output to calculate QFLUX.

We turn the ocean heat transport feedback off by setting the ocean heat transport convergence to its average value, for each month, from the first 10 yr of the NCAR CCSM run for the IPCC AR4 $4 \times \text{CO}_2$ scenario (which we call the “LO OHT” case). We turn the ocean heat transport feedback on by setting the ocean heat transport convergence to its average value, for each month, from the last 10 yr of the NCAR CCSM run for the IPCC AR4 $4 \times \text{CO}_2$ scenario (which we call the “HI OHT” case).

b. Convective cloud feedback

To turn the convective cloud feedback on and off we use the following algorithm. At every interface between atmospheric levels, including the surface and the top of the atmosphere, CAM calculates the following radiative fluxes: full-sky upward flux [$F_f^\uparrow(k + 1/2)$], full-sky downward flux [$F_f^\downarrow(k + 1/2)$], clear-sky upward flux [$F_c^\uparrow(k + 1/2)$], and clear-sky downward flux [$F_c^\downarrow(k + 1/2)$]. CAM calculates the clear-sky fluxes by setting all of the cloud variables to zero and calling the radiation code a second time at each time step. Here we use the index $k + 1/2$ to denote a value at a level interface. We calculate the following quantities from the monthly output of a standard interactive CRF run:

$$\Delta F_0^\uparrow\left(k + \frac{1}{2}\right) = F_{f0}^\uparrow\left(k + \frac{1}{2}\right) - F_{c0}^\uparrow\left(k + \frac{1}{2}\right), \\ \Delta F_0^\downarrow\left(k + \frac{1}{2}\right) = F_{f0}^\downarrow\left(k + \frac{1}{2}\right) - F_{c0}^\downarrow\left(k + \frac{1}{2}\right),$$

where we use the subscript 0 to signify quantities from the standard run. We then perform forced-CRF CAM runs in which we calculate the full-sky fluxes in the following way:

$$F_f^\uparrow\left(k + \frac{1}{2}\right) = F_c^\uparrow\left(k + \frac{1}{2}\right) + \Delta F_0^\uparrow\left(k + \frac{1}{2}\right), \\ F_f^\downarrow\left(k + \frac{1}{2}\right) = F_c^\downarrow\left(k + \frac{1}{2}\right) + \Delta F_0^\downarrow\left(k + \frac{1}{2}\right).$$

That is, we allow CAM to calculate the clear-sky radiative fluxes [$F_c^\uparrow(k + 1/2)$ and $F_c^\downarrow(k + 1/2)$] at each time step, but force the full-sky fluxes [$F_f^\uparrow(k + 1/2)$ and $F_f^\downarrow(k + 1/2)$] at each time step to be the sum of the clear-sky fluxes at each time step and the monthly mean flux differences that we saved from the standard run [$\Delta F_0^\uparrow(k + 1/2)$ and $\Delta F_0^\downarrow(k + 1/2)$]. In this way we apply the radiative effects of clouds at every level throughout the atmosphere, rather than just at the surface or top of the atmosphere.

We turn the convective cloud feedback off by using $\Delta F_0^\uparrow(k + 1/2)$ and $\Delta F_0^\downarrow(k + 1/2)$ values derived from the first 10 yr of the NCAR CCSM run for the IPCC

AR4 $4 \times \text{CO}_2$ scenario (which we call the “LO CRF” case). We turn the convective cloud feedback on by using $\Delta F_0^\uparrow(k+1/2)$ and $\Delta F_0^\downarrow(k+1/2)$ values derived from the last 10 yr of the NCAR CCSM run for the IPCC AR4 $4 \times \text{CO}_2$ scenario (which we call the “HI CRF” case).

Because we wish to isolate the effects of the convective cloud feedback, we only apply this forcing north of 60°N , which eliminates the remote effects that changes in low-latitude cloud radiative forcing can have on high-latitude climate (see Vavrus 2004). We also only apply the cloud radiative forcing between November and February, when the convective cloud feedback is most active (see section 3 and Fig. 6b). During this period, the region north of 60°N is in polar night, or nearly so, throughout November–February, which leads to zero or exceedingly small shortwave cloud radiative forcing. This allows us to apply the above method only to the longwave radiation, and not to the shortwave radiation.

By directly fixing the cloud radiative forcing, rather than the clouds themselves, we isolate the cloud radiative forcing effect in which we are interested. We also eliminate issues related to the nonlinearity of the cloud–radiation interaction, which would necessitate saving and applying cloud fields at the radiation time step (Langen and Caballero 2007). A disadvantage of our method is that changes in surface temperature can change radiative fluxes and CRF even if the optical thickness of the atmosphere remains constant.

The code we used to fix the longwave cloud radiative forcing in CAM is available online (see http://swell.eps.harvard.edu/~abbot/cam_mods.tgz).

c. Consistency tests

We find that the climate CAM produces when run at a CO_2 concentration of 280 ppm with ocean heat transport and cloud radiative forcing prescribed to their LO OHT and LO CRF values using the methods described above is very similar to the climate of the first 10 yr of the NCAR CCSM run for the IPCC AR4 $4 \times \text{CO}_2$ scenario. We also find that the climate CAM produces when run at a CO_2 concentration of 1120 ppm with ocean heat transport and cloud radiative forcing prescribed to their HI OHT and HI CRF values using the methods described above is very similar to the climate of the last 10 yr of the NCAR CCSM run for the IPCC AR4 $4 \times \text{CO}_2$ scenario. There is almost no sea ice in the Arctic at any point during the year when CAM is run with $\text{CO}_2 = 1120$ ppm, HI OHT, and HI CRF, which reproduces the most important feature (for this paper) of the NCAR CCSM run for the IPCC AR4 $4 \times \text{CO}_2$ scenario. We therefore conclude that the method we use to specify the ocean heat transport and cloud radiative forcing in CAM is internally consistent and the

mixed layer approximation we use to model the ocean is acceptable for our purposes.

REFERENCES

- Abbot, D. S., and E. Tziperman, 2008a: A high-latitude convective cloud feedback and equable climates. *Quart. J. Roy. Meteor. Soc.*, **134**, 165–185, doi:10.1002/qj.211.
- , and —, 2008b: Sea ice, high-latitude convection, and equable climates. *Geophys. Res. Lett.*, **35**, L03702, doi:10.1029/2007GL032286.
- , and —, 2009: Controls on the activation and strength of a high-latitude convective cloud feedback. *J. Atmos. Sci.*, **66**, 519–529.
- , M. Huber, G. Bousquet, and C. C. Walker, 2009: High- CO_2 cloud radiative forcing feedback over both land and ocean in a global climate model. *Geophys. Res. Lett.*, **36**, L05702, doi:10.1029/2008GL036703.
- Archer, D., and V. Brovkin, 2008: The millennial atmospheric lifetime of anthropogenic CO_2 . *Climatic Change*, **90**, 283–297.
- Bitz, C. M., P. R. Gent, R. A. Woodgate, M. M. Holland, and R. Lindsay, 2006: The influence of sea ice on ocean heat uptake in response to increasing CO_2 . *J. Climate*, **19**, 2437–2450.
- Briegleb, B. P., E. C. Hunke, C. M. Bitz, W. H. Lipscomb, M. M. Holland, J. L. Schramm, and R. E. Moritz, 2004: The sea ice simulation of CCSM2. NCAR Tech. Rep. NCAR-TN-455, 34 pp.
- Budyko, M. I., 1969: The effect of solar radiation variations on the climate of the Earth. *Tellus*, **21**, 611–619.
- Caballero, R., and P. L. Langen, 2005: The dynamic range of poleward energy transport in an atmospheric general circulation model. *Geophys. Res. Lett.*, **32**, L02705, doi:10.1029/2004GL021581.
- Eisenman, E., C. Bitz, and E. Tziperman, 2009: Rain driven by receding ice sheets as a cause of past climate change. *Paleoceanography*, in press, doi:10.1029/2009PA001778.
- Eisenman, I., 2007: Arctic catastrophes in an idealized sea ice model. 2006 Program of Studies: Ice, Woods Hole Oceanographic Institution Geophysical Fluid Dynamics Program Tech. Rep. 2007-02, 133–161. [Available online at <http://www.gps.caltech.edu/~ian/publications/Eisenman-2007.pdf>.]
- , and J. S. Wettlaufer, 2009: Nonlinear threshold behavior during the loss of Arctic sea ice. *Proc. Natl. Acad. Sci. USA*, **106**, 28–32.
- , N. Untersteiner, and J. S. Wettlaufer, 2007: On the reliability of simulated Arctic sea ice in global climate models. *Geophys. Res. Lett.*, **34**, L10501, doi:10.1029/2007GL029914.
- Forster, P., and Coauthors, 2007: Changes in atmospheric constituents and in radiative forcing. *Climate Change 2007: The Physical Science Basis*, S. Solomon et al., Eds., Cambridge University Press, 129–234.
- Francis, J. A., E. Hunter, J. R. Key, and X. Wang, 2005: Clues to variability in Arctic minimum sea ice extent. *Geophys. Res. Lett.*, **32**, L21501, doi:10.1029/2005GL024376.
- Graversen, R. G., T. Mauritsen, M. Tjernstrom, E. Kallen, and G. Svensson, 2008: Vertical structure of recent Arctic warming. *Nature*, **451**, 53–56.
- Holland, M. M., and C. M. Bitz, 2003: Polar amplification of climate change in coupled models. *Climate Dyn.*, **21** (3–4), 221–232.
- , —, and B. Tremblay, 2006: Future abrupt reductions in the summer Arctic sea ice. *Geophys. Res. Lett.*, **33**, L23503, doi:10.1029/2006GL028024.

- Huber, M., and L. C. Sloan, 1999: Warm climate transitions: A general circulation modeling study of the Late Paleocene Thermal Maximum (~56 ma). *J. Geophys. Res.*, **104**, 16 633–16 655.
- Intrieri, J. M., C. W. Fairall, M. D. Shupe, P. O. G. Persson, E. L. Andreas, P. S. Guest, and R. E. Moritz, 2002a: An annual cycle of Arctic surface cloud forcing at SHEBA. *J. Geophys. Res.*, **107**, 8039, doi:10.1029/2000JC000439.
- , M. D. Shupe, T. Uttal, and B. J. McCarty, 2002b: An annual cycle of Arctic cloud characteristics observed by radar and lidar at SHEBA. *J. Geophys. Res.*, **107**, 8030, doi:10.1029/2000JC000423.
- Kirk-Davidoff, D. B., and J.-F. Lamarque, 2008: Maintenance of polar stratospheric clouds in a moist stratosphere. *Climate Past*, **4**, 69–78.
- , D. P. Schrag, and J. G. Anderson, 2002: On the feedback of stratospheric clouds on polar climate. *Geophys. Res. Lett.*, **29**, 1556, doi:10.1029/2002GL014659.
- Langen, P. L., and R. Caballero, 2007: Cloud variability, radiative forcing and meridional temperature gradients in a general circulation model. *Tellus*, **59A**, 641–649, doi:10.1111/j.1600-0870.2007.00265.x.
- Lenke, P., and Coauthors, 2007: Observations: Changes in snow, ice and frozen ground. *Climate Change 2007: The Physical Science Basis*, S. Solomon et al., Eds., Cambridge University Press, 337–383.
- McBean, G., and Coauthors, 2005: Arctic climate: Past and present. *Arctic Climate Impact Assessment*, C. Symon, L. Arris, and B. Heal, Eds., Cambridge University Press, 22–60.
- Peters, R. B., and L. C. Sloan, 2000: High concentrations of greenhouse gases and polar stratospheric clouds: A possible solution to high-latitude faunal migration at the latest Paleocene thermal maximum. *Geology*, **28**, 979–982.
- Pierrehumbert, R. T., 2002: The hydrologic cycle in deep-time climate problems. *Nature*, **419**, 191–198.
- Ridley, J., J. Lowe, and D. Simonin, 2007: The demise of Arctic sea ice during stabilisation at high greenhouse gas concentrations. *Climate Dyn.*, **30**, 333–341.
- Schweiger, A. J., R. W. Lindsay, S. Vavrus, and J. A. Francis, 2008: Relationships between Arctic sea ice and clouds during autumn. *J. Climate*, **21**, 4799–4810.
- Sellers, W. D., 1969: A global climate model based on the energy balance of the earth–atmosphere system. *J. Appl. Meteor.*, **8**, 392–400.
- Serreze, M. C., M. M. Holland, and J. Stroeve, 2007: Perspectives on the Arctic's shrinking sea-ice cover. *Science*, **315**, 1533–1536.
- Sloan, L. C., and D. Pollard, 1998: Polar stratospheric clouds: A high latitude warming mechanism in an ancient greenhouse world. *Geophys. Res. Lett.*, **25**, 3517–3520.
- , J. C. G. Walker, T. C. Moore, D. K. Rea, and J. C. Zachos, 1992: Possible methane induced polar warming in the early Eocene. *Nature*, **357**, 320–322.
- , M. Huber, and A. Ewing, 1999: Polar stratospheric cloud forcing in a greenhouse world: A climate modeling sensitivity study. *Reconstructing Ocean History: A Window into the Future*, F. Abrantes and A. Mix, Eds., Kluwer Academic/Plenum, 273–293.
- Smetacek, V., and S. Nicol, 2005: Polar ocean ecosystems in a changing world. *Nature*, **437**, 362–368.
- Solomon, A., 2006: Impact of latent heat release on polar climate. *Geophys. Res. Lett.*, **33**, L07716, doi:10.1029/2005GL025607.
- Stern, H. L., R. W. Lindsay, C. M. Bitz, and P. Hezel, 2008: What is the trajectory of arctic sea ice? *Arctic Sea Ice Decline: Observations, Projections, Mechanisms, and Implications*, *Geophys. Monogr.*, Vol. 180, Amer. Geophys. Union, 175–185.
- Stroeve, J., M. M. Holland, W. Meier, T. Scambos, and M. Serreze, 2007: Arctic sea ice decline: Faster than forecast. *Geophys. Res. Lett.*, **34**, L09501, doi:10.1029/2007GL029703.
- Vavrus, S., 2004: The impact of cloud feedbacks on Arctic climate under greenhouse forcing. *J. Climate*, **17**, 603–615.
- , D. Waliser, A. Schwiger, and J. Francis, 2008: Simulations of 20th and 21st century Arctic cloud amount in the global climate models assessed in the IPCC AR4. *Climate Dyn.*, in press, doi:10.1007/s00382-008-0475-6.
- Winton, M., 2006: Does the Arctic sea ice have a tipping point? *Geophys. Res. Lett.*, **33**, L23504, doi:10.1029/2006GL028017.
- , 2008: Sea ice-albedo feedback and nonlinear arctic climate change. *Arctic Sea Ice Decline: Observations, Projections, Mechanisms, and Implications*, *Geophys. Monogr.*, Vol. 180, Amer. Geophys. Union, 111–131.